

Structural, dielectric and conductivity properties of Ba²⁺ doped (Bi_{0.5}Na_{0.5})TiO₃ ceramic

Meera Rawat, K. L. Yadav*, Amit Kumar, Piyush Kumar Patel, Nidhi Adhlakha, Jyoti Rani

Smart Materials Research Laboratory, Department of Physics, Indian Institute of Technology Roorkee, Roorkee 247667, India

*Corresponding author. Tel/Fax: (+91) 1332-273560; E-mail: klyadav35@yahoo.com

Received: 09 January 2012, Revised: 12 February 2012, Accepted: 28 April 2012

ABSTRACT

Polycrystalline (Bi_{0.5}Na_{0.5})_{1-x}Ba_xTiO₃ [here after BNBT], $x = 0, 0.02, 0.04, 0.06, 0.08,$ and 0.1 ceramics have been synthesized by conventional solid state reaction process and were characterized by X-ray diffraction technique, which indicates that on substitution of Ba²⁺ in Bi_{0.5}Na_{0.5}TiO₃ (BNT) ceramic there is splitting of the (2 0 0) peak for $x \geq 0.06$. This splitting in the peak position reveals that the composition BNBT-0.06 is well in Morphotropic Phase Boundary (MPB) region where rhombohedral and tetragonal phase co-exist. Scanning electron micrograph shows decrease in grain size from 0.66 to $0.53 \mu\text{m}$ with increasing concentration of Ba²⁺; and the dielectric constant of Ba²⁺ doped BNT ceramics increased with decreasing grain sizes and a maximum value was attained at size of $0.54 \sim 0.56 \mu\text{m}$. Doped BNT ceramic also exhibit diffuse phase transition and are characterised by a strong temperature and frequency dispersion of the permittivity which would be connected with the cation disorder in A-site of perovskite unit cell. Complex impedance spectroscopy is used to analyze the electrical behaviour of BNBT, which indicates the presence of grain effect and the composition exhibits Negative Temperature coefficient of resistance (NTCR) behaviour. The compounds exhibit Arrhenius type of electrical conductivity and the presence of non-Debye type of relaxation has been confirmed from impedance analysis. Copyright © 2012 VBRI Press.

Keywords: Ceramics; X-ray diffraction; grain size; complex impedance spectroscopy; NTCR behavior.



Meera Rawat did her postgraduate (2007) in physics from “Thakur Dev Singh Bisht Campus, Nainital” (Kumaon University), Uttarakhand. Currently she is doing Ph.D. in Physics (Experimental condensed matter) in Indian Institute of Technology Roorkee, India.



K. L. Yadav is currently Associate Professor in the Department of Physics, Indian Institute of Technology Roorkee, India. He is born and brought at Kharagpur, West Bengal, India and hold M.Sc. and Ph.D. degree in Physics from Indian Institute of Technology Kharagpur, India in 1989 and 1994, respectively. In 2001, he became BOYSCAST Fellow at Materials Research Institute, Pennstate University, USA. In addition, he obtained JSPS fellowship at National Institute for Materials Science, Tsukuba, Japan in 2010. In his academic carrier, he has published more than 93 papers in SCI Journals, presented about 27 papers in various conferences/symposia and is an author of two contributory chapters in books of International level in the field of materials science and technology. His major research interests are Functional Nanomaterials, Multiferroics, Sensors and Biomaterials. His recent research interest is focused on designing and development of the smart materials for

device applications. Dr. Yadav strongly advocates the use of research methodology in the education.



Amit Kumar is completed his postgraduation in the Physics from ‘Chaudhary Charan Singh University Meerut’ in the year of 2005. Then he worked as Junior Reseach Fellow and Project Associate at I.I.T. Bombay and I.I.T. Delhi, respectively. Currently he is going to submit Ph.D. thesis under the guidance of Dr. K. L. Yadav in Indian Institute of Technology Roorkee, India. He has published more than 10 international papers in reputed journal such as; Journal of alloys and Compounds, Advance Science Letters, and Material Chemistry and Physics.

Introduction

Lead oxide based ferroelectrics such as PZT, are of technological importance because of their wide applications in transducers, actuators, and microelectronic devices [1–3]. The toxicity of lead raised serious environmental concerns and the restriction of use of lead in electronic devices. Recently, much attention has been given to the research on new lead-free piezoelectric materials because of the concern regarding the detrimental effect of lead on environment [4–6]. Bismuth sodium

titanate, $(\text{Bi}_{1/2}\text{Na}_{1/2})\text{TiO}_3$ (abbreviated to BNT), is an attractive lead-free A-site complex perovskite for high T_c ferroelectric relaxor material used to replace lead-contented perovskite materials because of the lead-free control of sintering atmosphere and lack of lead pollution during the process of preparation. Ferroelectric bismuth sodium titanate $(\text{Bi}_{1/2}\text{Na}_{1/2})\text{TiO}_3$, discovered by Smolenski et al, is the compound that has been most widely studied [7]. Ferroelectric materials of the perovskite family (ABO₃-type) have received considerable attentions for the past several years owing to their promising potentials for various electronic devices such as multilayer capacitors (MLCCs), piezoelectric transducers, pyroelectric detectors/sensors, electrostrictive actuators, precision micropositioners, MEMS (Micro-Electro-Mechanical Systems), etc. BNT has been considered to be a good candidate of lead-free piezoelectric ceramics because of its strong ferroelectricity at room temperature and high Curie temperature T_c of 320 °C [8–13]. However, pure BNT suffers from a large coercive field $E_C = 73\text{kVcm}^{-1}$ at room temperature as well as a rhombohedral to tetragonal phase transition below the Curie point, [14] both of which limit its usefulness in the transducer industry. Also pure BNT ceramics are limited by some of its other shortcomings in electric properties, for example: low relative dielectric permittivity (ϵ_r), narrow sintering temperature range and high conductivity at room temperature [15]. Sodium bismuth titanate is a compound with strong ferroelectricity but these ceramics are difficult to pole and to sinter. Thus the pure BNT ceramic usually exhibits weak piezoelectric properties [16]. To improve the poling process and enhance the piezoelectric properties of the BNT ceramics, a number of BNT-based solid solutions, such as BNT-BaTiO₃ [17,18], BNT-(Ba,Sr)TiO₃ [19], BNT-Bi_{0.5}K_{0.5}TiO₃ [9], BNT-SrTiO₃-Bi_{0.5}Li_{0.5}TiO₃ [20], BNT-Bi_{0.5}K_{0.5}TiO₃-Bi_{0.5}Li_{0.5}TiO₃ [21], BNT-Bi_{0.5}K_{0.5}TiO₃-BiFeO₃ [22], BNT-BT-Bi_{0.5}K_{0.5}TiO₃ [23], BNT-BT-KNbO₃ [24], and Bi₂O₃ doped BNT-BaTiO₃ [25] have been developed and studied in recent years. The $(1-x)(\text{Bi}_{1/2}\text{Na}_{1/2})\text{TiO}_3-x\text{BaTiO}_3$ system has been of great interest since the discovery of an MPB. In 1993, Takenaka [26] reported that BNBT6 ceramics, which is near the MPB, has relatively good piezoelectric properties, and since then, much research has focused on the BNBT6-system and good properties have been obtained [27–29]. Rare earth oxide was often used as an additive in order to improve the structural, electrical properties of piezoelectric and ferroelectric ceramics, recently of them are WO₃ [30], Dy₂O₃ [31], CeO₂ [32, 33], Y₂O₃ [34], and La₂O₃ [35] have been tested to further modify piezoelectric properties of BNBT6 ceramics.

Most of the work that has been carried out in BNBT system is in its preparative methods, dielectric (variation of ϵ' with temperature) Ferroelectric and piezoelectric properties. Further, in ferroelectrics in general, the study of electrical conductivity is very important since the associated physical properties like piezoelectricity, pyroelectricity and also strategy for poling are dependent on the order and nature of conductivity in these materials. In this paper we present systematic study of structural and

dielectric properties of $(\text{Bi}_{0.5}\text{Na}_{0.5})_{1-x}\text{Ba}_x\text{TiO}_3$ (BNBT) and also present complex impedance studies of BNBT ceramics to understand the mechanism of charge transport and role of grains on electrical properties of ceramics.

Experimental

$(\text{Bi}_{0.5}\text{Na}_{0.5})_{1-x}\text{Ba}_x\text{TiO}_3$ (with $x = 0, 0.02, 0.04, 0.06, 0.08$ and 0.1) polycrystalline ceramics were prepared by conventional solid-state reaction method, using required amount of analytic grade reagents Bi₂O₃ (99.5%, Himedia, India), Na₂CO₃ (99.9%, Qualigens, India) BaCO₃ (98.5%, Himedia, India) and TiO₂ (99%, Himedia, India) as starting materials. The weighed powders in stoichiometric ratios were ground well in agate mortar in acetone medium for 4 h. An extra amount of 3 wt% Bi₂O₃ and Na₂CO₃ were added to initial mixture to compensate the losses of bismuth and sodium (offset A-site cations) which evaporate at high temperature. The resultant mixture was calcined at 1323 K for 2h. The phase purity of the final product was confirmed via the X-Ray diffraction (XRD) technique with Cu (K_α) ($\lambda = 1.5402 \text{ \AA}$) radiation, over a wide range of Bragg angle ($20^\circ \leq 2\theta \leq 70^\circ$) with a scanning speed of 1° min^{-1} , using BRUKER D8 XRD Spectroscopy. The calcined powders were ground again until the grains reached to a fine form and then pressed into pellets with diameter of 8-9 mm and thickness of 1-1.2 mm by Hydraulic press. These pellets were sintered at 1373 K for 2 h and then slowly cooled down to room temperature. Sintered pellets were painted with silver paste on both surfaces in order to measure their electric properties. Field emission scanning electron microscope (FESEM) coupled with Energy dispersive X-ray Spectroscopy (EDAX) was used to analyse the microstructure and to check the chemical composition of the ceramic samples. The densities of the sintered pellets have been determined by the liquid displacement/Archimedes method. The permittivity (ϵ'), loss tangent ($\tan\delta$), and complex impedance analysis was carried out using a LCR Hi-tester (model 3532-50 HIOKI) as a function of temperature and frequency.

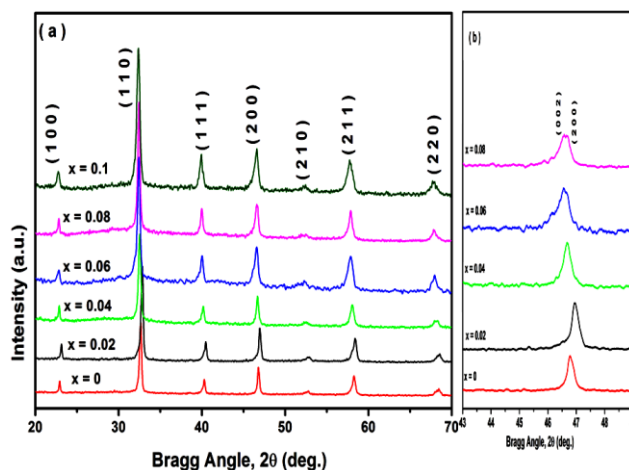


Fig. 1. X-ray diffraction pattern for various compositions in the system $(\text{Bi}_{0.5}\text{Na}_{0.5})_{1-x}\text{Ba}_x\text{TiO}_3$ for (a) $2\theta, 20^\circ\text{--}70^\circ$ and (b) $2\theta, 43^\circ\text{--}49^\circ$.

Results and discussion

Crystal structure and density

Fig. 1(a) shows the XRD pattern of the sintered $(\text{Bi}_{0.5}\text{Na}_{0.5})_{1-x}\text{Ba}_x\text{TiO}_3$ ($x = 0, 0.02, 0.04, 0.06, 0.08, 0.1$) ceramics. It shows the formation of single-phase compounds with rhombohedral structure. With the increase of Ba^{2+} concentration, the diffraction peak 2θ angle decreased gradually indicating the increase in the volume of the unit cell because of Ba^{2+} (1.39 Å) which is substituted for the smaller ionic radii of Na^+ (1.18 Å) and Bi^{3+} (1.17 Å). Also, the substitution of Ba^{2+} in BNT for $x \geq 0.06$ resulted in a splitting of the (2 0 0) peak into two peaks of (0 0 2) and (2 0 0) reflections as seen in inset **Fig. 1(b)**. This splitting in the peak position reveals the composition BNBT-0.06 is well in MPB region where rhombohedral and tetragonal phase co-exist [36-38].

Table 1. Lattice parameters of $(\text{Bi}_{0.5}\text{Na}_{0.5})_{1-x}\text{Ba}_x\text{TiO}_3$ ceramics.

Composition	BNBT1 $x=0$	BNBT2 $x=0.02$	BNBT3 $x=0.04$	BNBT4 $x=0.06$	BNBT5 $x=0.08$	BNBT6 $x=0.1$
Lattice parameter a (Å)	3.8521	3.8819	3.8848	3.8754	3.8872	3.8727
Distortion (angle)	89.7513	89.9882	89.9312	89.7525	89.8479	89.7491

Calculated value of lattice parameters are given in **Table 1**. The experimental densities are found to be in between 92-95% to that of theoretical values. FE-SEM micrograph **Fig. 2(a-f)** shows spherical shaped grains. It was used to determine the grain size of sintered pellets. The average grain size (~ 0.5 - $0.7 \mu\text{m}$) was determined by linear interception method. SEM images shows that the grain size of Ba^{2+} doped BNT compositions are smaller than undoped BNT, which prove that Ba^{2+} in BNT act as the grain growth inhibitor and prohibit further growth of grains. Energy dispersive X-ray analysis (EDS) (**Fig. 2g**) confirmed that all the samples are in stoichiometry ratio.

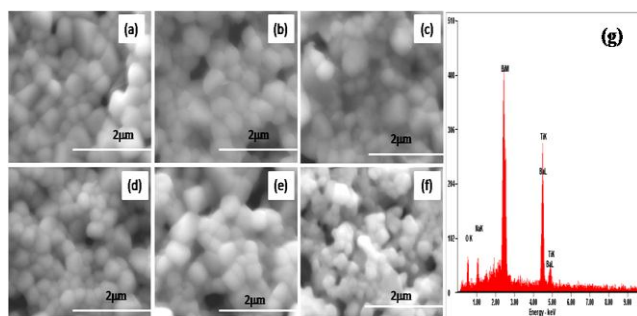


Fig. 2. SEM Micrograph for (a) $x = 0$, (b) $x = 0.02$, (c) $x = 0.04$, (d) $x = 0.06$, (e) $x = 0.08$, and (f) $x = 0.1$ in the system $(\text{Bi}_{0.5}\text{Na}_{0.5})_{1-x}\text{Ba}_x\text{TiO}_3$ (g) Energy dispersive X-ray spectrum for $(\text{Bi}_{0.5}\text{Na}_{0.5})_{1-x}\text{Ba}_x\text{TiO}_3$.

Dielectric behavior

Fig. 3(a, b), respectively, shows the frequency dependence of dielectric permittivity ϵ' and dielectric loss ϵ'' ($\tan\delta$) at room temperature, both follow inverse dependence on frequency, normally followed by almost all ferroelectric materials. The dielectric permittivity ϵ' of a material has four polarization contributions: electronic polarization, dipolar polarization, ionic polarization, and space charge polarization. Response frequencies for electronic and ionic polarization are $\sim 10^{16}$ and 10^{13} Hz respectively and at a

frequency of 10 kHz, contribution from space charge polarization is likely to be dominant. **Fig. 3(b)** shows the variation of dielectric loss with frequency at room temperature. It is observed that with increasing frequency dielectric loss decreases rapidly and after 10 kHz it is almost constant. This can be understood in term of space charge polarization in materials. In these materials defects, distortions are cause for dielectric loss.

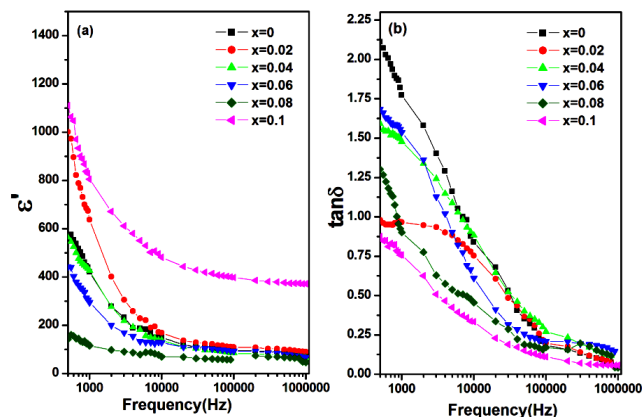


Fig. 3. Variation of (a) ϵ' and (b) $\tan\delta$ with frequencies for various compositions in the system $(\text{Bi}_{0.5}\text{Na}_{0.5})_{1-x}\text{Ba}_x\text{TiO}_3$.

Fig. 4 shows the temperature-dependent dielectric permittivity and **Fig. 5** shows variation of dielectric loss with temperature of the BNBT ($x=0, 0.02, 0.04, 0.06, 0.08, 0.1$) ceramics for the frequency range from 1kHz-1MHz. The temperature (T_m) or Curie point (T_c) corresponds to the maximum value of dielectric permittivity. It can be seen that both ϵ' and ϵ'' are strongly frequency dependent, and we find that dielectric permittivity increases as the concentration of Ba^{2+} increased and it is maximum for $x = 0.08$, this increase in dielectric permittivity depends on decrease in grain size and maximum value attained for the grain size $0.54 \mu\text{m}$ for $x = 0.08$. According to Arlt et al. [39], this is consequence of the decrease of the 90° domain width decreasing the grain size. The multiple ion occupation at different sites causes deviation from normal Curie-Weiss behaviour, where T_m is not sharp, but physical properties change rather gradually over a temperature range, which is referred as diffused phase transition. This indicate that BNBT ceramics are relaxor like, due to complex occupation of Ba^{2+} , Na^+ , and Bi^{3+} cations at A-site. In most of the composition higher dielectric permittivity at lower frequency is usually attributed to space charges which exist in BNT composition with A-site deficiency serving as charged vacancies [40]. These vacancies in stoichiometry composition are due to evaporation of A-site cations at high temperature. However this evaporation of A-site elements can be offset by the excess addition of Bi^{3+} and Na^+ ions.

A modified Curie-Weiss law has been proposed to quantify the diffuseness of a phase transition at T_m [41, 42],

$$(1/\epsilon' - 1/\epsilon'_{max}) = A(T - T_m)^\gamma \quad (1)$$

where γ is a critical exponent which lie in the range $1 < \gamma \leq 2$. $\gamma = 1$ represents ideal Curie-Weiss behaviour while

between 1 and 2 indicate diffuse behaviour [43]. We determined the value of γ from the slope of straight line fitted to the logarithmic plots of reciprocal permittivity $(1/\epsilon' - 1/\epsilon'_{max})$ measured at 1 KHz as a function of $(T - T_m)$ as show in Fig. 6. There is increase in diffusive factor (γ) as we increase the concentration of Ba^{2+} in BNT. These results imply an elevation of the relaxor feature and transition from normal ferroelectric to relaxor ferroelectrics.

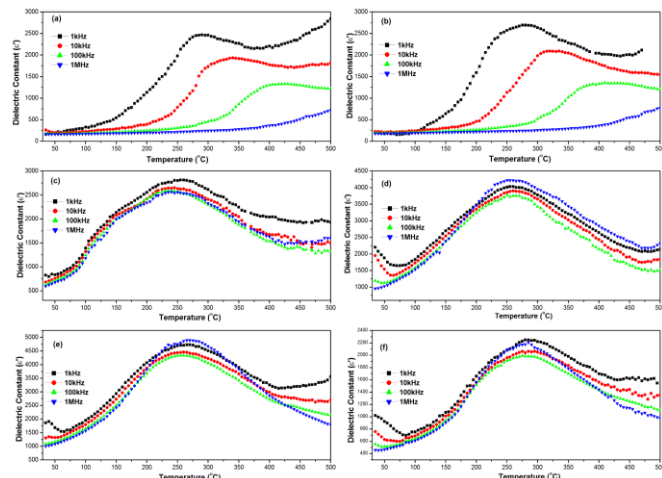


Fig. 4. Variation of dielectric constant (ϵ') with temperature at different frequencies for (a) $x = 0$, (b) $x = 0.02$, (c) $x = 0.04$, (d) $x = 0.06$, (e) $x = 0.08$, and (f) $x = 0.1$ respectively in system $(Bi_{0.5}Na_{0.5})_{1-x}Ba_xTiO_3$.

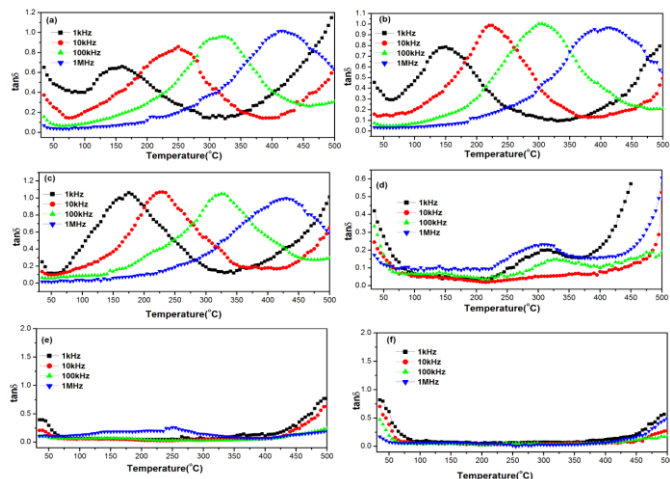


Fig. 5. Variation of dielectric loss ($\tan\delta$) with temperature at different frequencies for (a) $x = 0$, (b) $x = 0.02$, (c) $x = 0.04$, (d) $x = 0.06$, (e) $x = 0.08$, and (f) $x = 0.1$ respectively in system $(Bi_{0.5}Na_{0.5})_{1-x}Ba_xTiO_3$.

Impedance analysis

Fig. 7 shows the variation of the real part of impedance Z' with frequency from 100Hz-1MHz in temperature range from 30-500 °C. It is observed that the value of Z' decreases with increase in temperature as well as frequency which shows that BNBT has the negative temperature coefficient of resistance (NTCR). This indicates an increase in ac conductivity with increase in temperature and frequency.

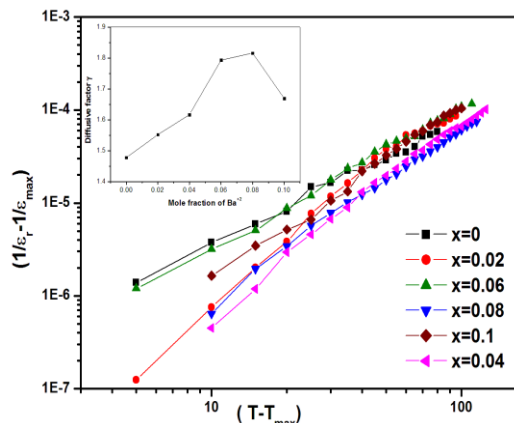


Fig. 6. Variation of $(1/\epsilon' - 1/\epsilon'_{max})$ with $(T - T_{max})$ for various compositions in the system $(Bi_{0.5}Na_{0.5})_{1-x}Ba_xTiO_3$ (inset shows variation of diffusive factor with mole fraction of Ba^{2+}).

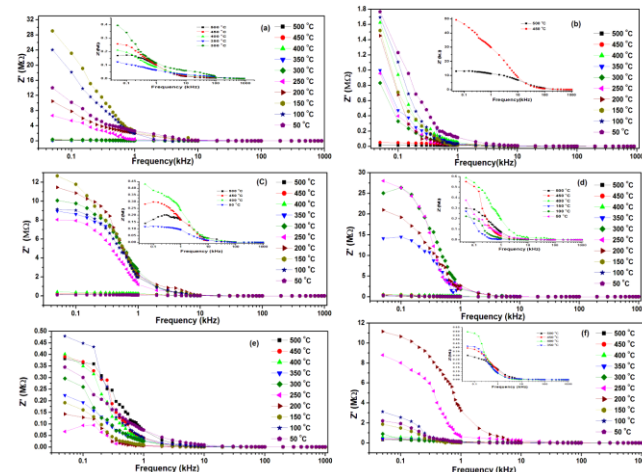


Fig. 7. Variation of Z' with frequency at different temperature for (a) $x = 0$, (b) $x = 0.02$, (c) $x = 0.04$, (d) $x = 0.06$, (e) $x = 0.08$, and (f) $x = 0.1$ respectively in system $(Bi_{0.5}Na_{0.5})_{1-x}Ba_xTiO_3$ (insets in all figure show enlarged view of Z' vs frequency plots at higher temperature).

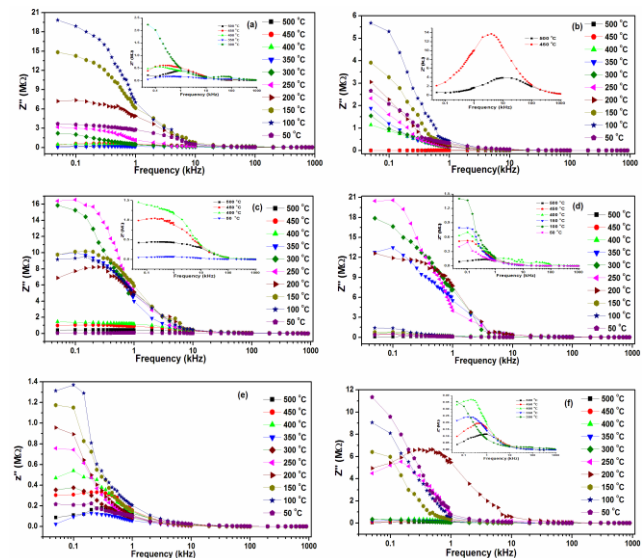


Fig. 8. Variation of Z'' with frequency at different temperature for (a) $x = 0$, (b) $x = 0.02$, (c) $x = 0.04$, (d) $x = 0.06$, (e) $x = 0.08$, and (f) $x = 0.1$ respectively in system $(Bi_{0.5}Na_{0.5})_{1-x}Ba_xTiO_3$ (insets in all figure show enlarged view of Z'' vs. frequency plots at higher temperature).

Fig. 8 shows the plot of imaginary part of impedance Z'' or impedance loss spectrum with frequency at different temperatures (50-500 °C). At lower temperatures Z'' decreased monotonically. There is asymmetric peak broadening (inset of Fig. 8) and the decrease of value of Z'' with increasing temperature and peak shifted toward higher frequency. The asymmetric broadening of peaks in frequency explicit plots of Z'' indicates the spreading of relaxation times, i.e. existence of a temperature dependent electrical relaxation phenomenon in the material. Complex impedance formalism helps in determining inter-particle interaction like, grain, grain boundary effects etc.

The temperature dependence of complex impedance spectrum Z' vs Z'' (called Nyquist plot) of BNBT compounds with $x = 0, 0.02, 0.04, 0.06, 0.08,$ and 0.1 is shown in **Fig. 9** over a wide frequency range for the temperature 450 °C, and 500 °C. It is observed that impedance data at room temperature do not take the shape of semicircle but rather resemble a straight line, which suggest the insulating behaviour of BNBT and with increase in temperature the slope of lines decreases, and line bend towards the real (Z') axis and at 450 °C, a semicircle could be traced, indicating the increase in conductivity of samples, it can be also observed that the peak maxima of the plots decrease and frequency for the maximum shift to higher values with increase in temperature. It is observed that all the semicircles arc exhibits some degree of depression indicating that centres of these semicircles lies below the real Z' axis, it showing presence of non-Debye type of relaxation in the material. The non-Debye type nature of dielectric relaxation could be analysed through complex impedance plots.

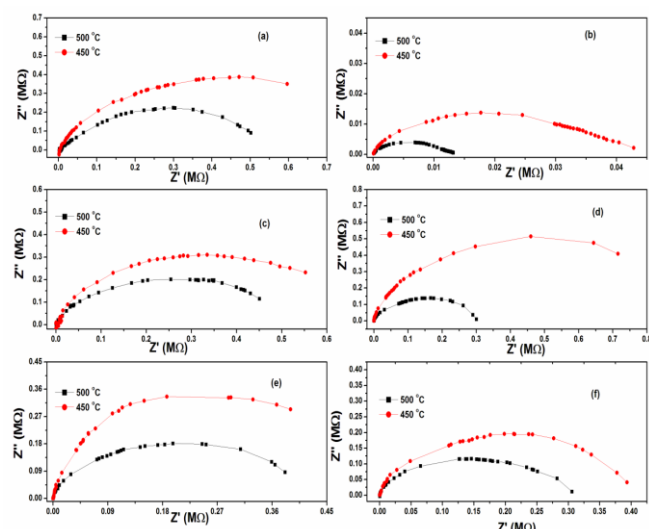


Fig. 9. Cole-Cole plots for (a) $x = 0$, (b) $x = 0.02$, (c) $x = 0.04$, (d) $x = 0.06$, (e) $x = 0.08$, and (f) $x = 0.1$ respectively in system $(\text{Bi}_{0.5}\text{Na}_{0.5})_{1-x}\text{Ba}_x\text{TiO}_3$ at 500 °C and 450 °C.

For Debye type relaxation, one expect semicircle plots with centre located on the real Z' axis, whereas for Non-Debye relaxation these argand plane plots are close to semicircle arc with end point on the real axis and centre lying below this axis. The complex impedance in such situation can be described as [44]

$$Z^*(\omega) = Z' - iZ'' = R/[1 + (i\omega/\omega_0)^{1-\alpha}] \quad (2)$$

where α represent the magnitude of departure of the electrical response from an ideal condition and can be determined from the location of the centre of the semicircles. When α goes to zero then equation (2) gives rise to classical Debye's formalism. Here it can be seen that complex impedance plots are not represented by full semicircle and centre lies below the real Z' axis, which suggests that dielectric relaxation is non-Debye type in BNBT. This may be due to the presence of distributed elements in the material-electrode system [45]. Also the value of α increases with rise in temperature. The correlation among the Debye relaxators may start developing via formation of non-polar clusters of Na-TiO_3 and Bi-TiO_3 . Since the relaxation times of relaxators within clusters are distributed over a wide spectrum at higher temperatures, their response to external field are in a different time domain. This results in the deviation from Cole-Cole plots. There is presence of single semicircular arc shown by plot indicates bulk or grain resistance effect come into force. The bulk resistance (R_b) obtained from the intercept on the Z' - axis, which decreases with the rise of temperature. This electrical behavior can be represented in terms of an equivalent circuit which consisting of series combination of parallel RC circuits. The bulk capacitance (C_b) was calculated using the relation:

$$\omega_{max} R_b C_b = 1 \quad (3)$$

where $\omega_{max} = 2\pi f_{max}$ is the angular frequency at the maxima of the semicircle due to grain effect in the complex impedance plots (**Fig. 9**). Variation of R_b and C_b of ceramic with temperature can be seen in **Fig. 10** in which the value of R_b decreases with temperature, this decrease in the value of R_b of BNBT is associated with the increase in conductivity with increase in temperature. This clearly indicates the negative temperature coefficient of resistance (NTCR) behaviour of the compounds [42, 46].

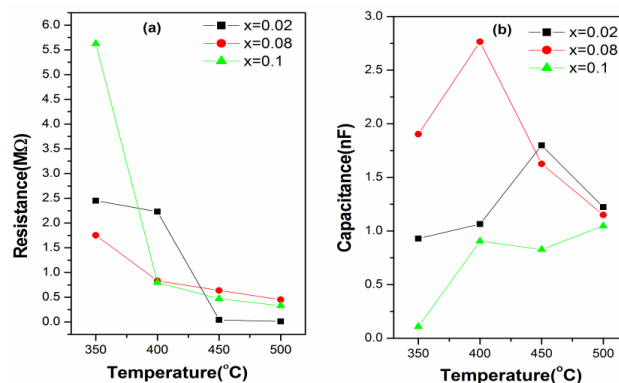


Fig. 10. Variation of (a) R_b and (b) C_b , with temperature for $x = 0.02$, $x = 0.08$, and $x = 0.1$ in the system $(\text{Bi}_{0.5}\text{Na}_{0.5})_{1-x}\text{Ba}_x\text{TiO}_3$.

The impedance loss spectra have been used to evaluate the relaxation time (τ) of the charge carriers by using the relation, $\omega_{max}\tau = 2\pi f_{max}\tau = 1$. The relaxation time basically gives an estimation of the dynamics of the

electrical relaxation process occurring in the material. Fig. 11(a) shows the variation of τ as a function of inverse of absolute temperature for different concentration of Ba doping in BNT.

It is found that higher the value of τ , the slower is the electrical relaxation process, and vice versa. The nature of variation of τ with temperature follows the Arrhenius relation;

$$\tau = \tau_0 \exp\left(-\frac{E_a}{K_B T}\right) \quad (4)$$

where τ_0 is the pre exponential factor, E_a the activation energy, K_B the Boltzmann constant and T is the absolute temperature.

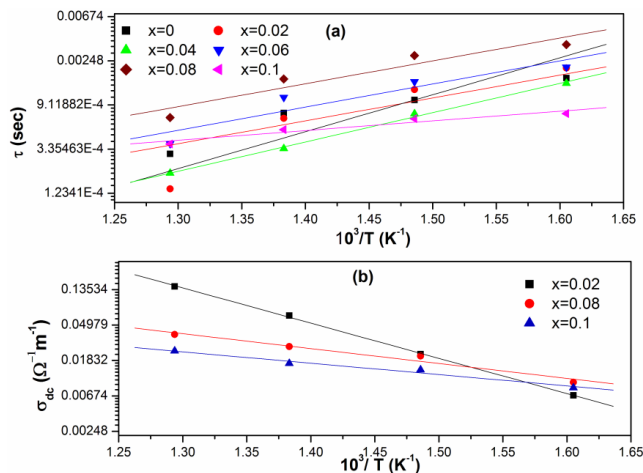


Fig. 11. Variation of (a) relaxation time τ and (b) dc conductivity (σ_{dc}), with ($10^3/T$) of $(\text{Bi}_{0.5}\text{Na}_{0.5})_{1-x}\text{Ba}_x\text{TiO}_3$ with $x = 0, x = 0.02, x = 0.04, x = 0.06, x = 0.08,$ and $x = 0.1$.

The value of activation energy of the samples evaluated from the linear fit to τ -plot is 0.45, 0.72, 0.52, 0.45, 0.44 and 0.19 eV for $x = 0.0, 0.02, 0.04, 0.06, 0.08$ and 0.1 , respectively. It is also shown that the value of activation energy firstly increases for $x = 0-0.02$ and thereafter it decreases with increasing Ba^{2+} contents. Fig. 11(b) shows the variation of dc electrical conductivity ($10^3/T$) of BNBT compound with temp follow the Arrhenius relation:

$$\sigma_{dc} = \sigma_0 \exp\left(-\frac{E_a}{K_B T}\right) \quad (5)$$

where all the symbols have their usual meanings. Using the above equation, the value of activation energy (E_a) of compound is 0.82, 0.39 and 0.21 for $x = 0.02, 0.08$ and 0.1 respectively, which are very close to the values obtained from τ -plots, these resemblance indicates that the relaxation and conductivity processes may be attributed to the same type of charge carriers [47].

Conclusion

In this paper we report the systematic study on structural, dielectric and electrical transport properties of $(\text{Bi}_{0.5}\text{Na}_{0.5})_{1-x}\text{Ba}_x\text{TiO}_3$ [BNBT] ceramics prepared by solid state reaction

method. The X-Ray powder diffraction pattern of materials have been indexed and found to be single phase with rhombohedral structure and also shows existence MPB for $x = 0.06$, where rhombohedral and tetragonal structure coexist. Scanning electron micrograph shows decrease in grain size with increasing concentration of Ba^{2+} , and the dielectric constant of Ba^{2+} doped BNT ceramics increased with decreasing grain sizes and a maximum value was attained at size of $0.54 \mu\text{m}$ for $x = 0.08$. Existence of diffuse phase transition in BNBT is mainly due to cation disorder in A-site of perovskite unit cell. The complex impedance or Nyquist plots indicates the presence of grain effect (bulk resistance), which is found to decrease with increase in temperature. It suggests that the composition exhibits the NTCR behaviour usually shown by semiconductors. The nature of electrical conductivity (dc) with temperature shows that the compound exhibit Arrhenius type of electrical conductivity and the dielectric relaxation in the system was found to be of non-Debye type.

Acknowledgement

We thanks to the Council of Scientific and Industrial Research (CSIR), New Delhi, India for financial support under the project grant 03(1156)/10/EMR 2nd dated 26-04-2010.

Reference

- Jaffe, B.; Cook, W. R.; and Jaffe, H.; *Piezoelectric Ceramics Academic, London*, **1971**, 271.
DOI: [10.1016/0022-460X\(72\)90684-0](https://doi.org/10.1016/0022-460X(72)90684-0)
- Haertling, G. H.; *J. Am. Ceram. Soc.*, **1999**, 82, 797.
DOI: [10.1111/j.1151-2916.1999.tb01840](https://doi.org/10.1111/j.1151-2916.1999.tb01840)
- Rödel, J.; Jo, W.; Seifert, K.; Anton, E. M.; Granzow, T.; and Damjanovic, D.; *J. Am. Ceram. Soc.* **2009**, 92, 1153.
DOI: [10.1111/j.1551-2916.2009.03061.x](https://doi.org/10.1111/j.1551-2916.2009.03061.x)
- Cross, E.; *Nature London* **2004**, 432, 24.
DOI: [10.1038/nature03142](https://doi.org/10.1038/nature03142)
- Saito, Y.; Takao, H.; Tani, T.; Nonoyama, T.; Takatori, K.; Homma, T.; Nagaya, T.; and Nakamura, M.; *Lead-free piezoceramics. Nature* **2004**, 432, 84.
DOI: [10.1038/nature03028](https://doi.org/10.1038/nature03028)
- Takenaka, T.; Nagata, H.; *J. Eur. Ceram. Soc.* **2005**, 25, 2693.
DOI: [10.1016/j.jeurceramsoc.2005.03.125](https://doi.org/10.1016/j.jeurceramsoc.2005.03.125)
- Smolenski, G.A.; Aganovskaya, A.I.; *Sov. Phys. Solid State* **1960**, 1, 1429.
- Dai, Y. J.; Pan, J. S.; Zhang, X. W.; *Key Eng. Mater.* **2007**, 336–338, 206.
DOI: [10.4028/www.scientific.net/KEM.336-338.206](https://doi.org/10.4028/www.scientific.net/KEM.336-338.206)
- Yang, Z. P.; Liu, B.; Wei, L. L.; Hou, Y. T.; *Mater. Res. Bull.* **2008**, 43, 81.
DOI: [10.1016/j.materresbull.2007.02.016](https://doi.org/10.1016/j.materresbull.2007.02.016)
- Takenaka, T.; Okuda, T.; Takegahara, K.; *Ferroelectrics* **1997**, 196, 175.
DOI: [10.1080/00150199708224156](https://doi.org/10.1080/00150199708224156)
- Wang, X. X.; Chan, H. L. W.; Choy, C. L.; *J. Am. Ceram. Soc.* **2003**, 86, 1809.
DOI: [10.1111/j.1151-2916.2003.tb03562.x](https://doi.org/10.1111/j.1151-2916.2003.tb03562.x)
- Nagata, H.; Koizumi, N.; Takenaka, T.; *Key Eng. Mater.* **1999**, 169–170, 37.
DOI: [10.4028/www.scientific.net/KEM.169-170.37](https://doi.org/10.4028/www.scientific.net/KEM.169-170.37)
- Nagata, H.; Yoshida, M.; Makiuchi, Y.; Takenaka, T.; *Jpn. J. Appl. Phys.* **2003**, 42, 7401.
DOI: [10.1143/JJAP.42.7401](https://doi.org/10.1143/JJAP.42.7401)
- Suchanicz, J.; Röleder, K.; Kwapiulinski, J.; and JankowskaSumara, I.; *Phase Transitions* **173** **1996**, 57, 173.
DOI: [10.1080/01411599608208744](https://doi.org/10.1080/01411599608208744)
- Lin, Y. H.; Zhao, S. J.; Cai, N.; Wu, J. B.; Zhou, X. S.; Nan, C. W.; *Mater. Sci. Eng. B* **2003**, 99, 449.
DOI: [10.1016/S0921-5107\(02\)00465-8](https://doi.org/10.1016/S0921-5107(02)00465-8)
- Herabut, A.; Safari, A.; *J. Am. Ceram. Soc.* **1997**, 80, 2954.
DOI: [10.1111/j.1151-2916.1997.tb03219.x](https://doi.org/10.1111/j.1151-2916.1997.tb03219.x)

17. Zhang, D. Z.; Zhenga, Feng, X.; Zhang, T.; Sun, J.; Dai, S. H.; Gong, L. J.; Gong, Y. Q.; He, L.; Zhu, Z.; Huang, J.; Xu, X.; *J. Alloys Compd.* **2010**, *504*, 129.
DOI: [10.1016/j.jallcom.2010.05.069](https://doi.org/10.1016/j.jallcom.2010.05.069)
18. DOI: [10.1016/j.jallcom.2010.05.069](https://doi.org/10.1016/j.jallcom.2010.05.069)
19. Ma, C.; Tan, X.; *Solid State Commun.*, **2010** 150,1497.
DOI: [10.1016/j.ssc.2010.06.006](https://doi.org/10.1016/j.ssc.2010.06.006)
20. Lee, W. C.; Huang, C. Y.; Tsao, L. K.; Wu, Y. C.; *J. Alloys Compd.* **2010**, *492* 307.
DOI: [10.1016/j.jallcom.2009.11.083](https://doi.org/10.1016/j.jallcom.2009.11.083)
21. Lin, D. M.; Kwok, K. W.; Chan, H. L. W.; *J. Alloys Compd.*, **2009**, *481*, 310.
DOI: [10.1016/j.jallcom.2009.02.120](https://doi.org/10.1016/j.jallcom.2009.02.120)
22. Yang, Z. P.; Hou, Y. T.; Pan, H.; Chang, Y. F.; *J. Alloys Compd.*, **2009**, *480*, 246.
DOI: [10.1016/j.jallcom.2009.02.030](https://doi.org/10.1016/j.jallcom.2009.02.030)
23. Zou, M. J.; Fan, H. Q.; Chen, L.; Yang, W. W.; *J. Alloys Compd.*, **2010**, *495* 280.
DOI: [10.1016/j.jallcom.2010.02.025](https://doi.org/10.1016/j.jallcom.2010.02.025)
24. Zhang, Shan-Tao; Yang, Bin; Cao, Wenwu; *Acta Materialia*, **2012**, *60*, 469.
DOI: [10.1016/j.actamat.2011.10.010](https://doi.org/10.1016/j.actamat.2011.10.010)
25. Ni, H.; Luo, L.; Li, W.; Zhu, Y.; Luo, H.; *J. Alloys Compd.*, **2011** 509, 3958.
DOI: [10.1016/j.jallcom.2010.12.190](https://doi.org/10.1016/j.jallcom.2010.12.190)
26. Liu, M. L.; Yang, D. A.; Qu, Y. F.; *J. Alloys Compd.* **2010**, *496*, 449.
DOI: [10.1016/j.jallcom.2010.01.160](https://doi.org/10.1016/j.jallcom.2010.01.160)
27. Takenaka, T.; Huzumi, A.; Hata, T.; Sakata, K.; *Silic. Indus.* **1993**, 7(8) 136.
28. Li, Hui-dong; Feng, Chu-de; Yao, Wen-long; *Mater. Lett.* **2004**, *58*, 1194.
DOI: [10.1016/j.matlet.2003.08.034](https://doi.org/10.1016/j.matlet.2003.08.034)
29. Shieh, J.; Wu, K. C.; Chen, C. S.; *Acta Mater.* **2007**, *55*, 3081.
DOI: [10.1016/j.actamat.2007.01.012](https://doi.org/10.1016/j.actamat.2007.01.012)
30. Lin, D.; Kwok, K. W.; Chan, H. L. W.; *Solid State Ionics*, **2008**, *178*, 1930.
DOI: [10.1016/j.ssi.2007.12.096](https://doi.org/10.1016/j.ssi.2007.12.096)
31. Sun, H.; Wang, X.; Yao, X.; *Ceramics International*, **2012**, *38S*, S373.
DOI: [10.1016/j.ceramint.2011.05.015](https://doi.org/10.1016/j.ceramint.2011.05.015)
32. Fu, P.; Xu, Z.; Chu, R.; Li, W.; Xie, Q.; Zhang, Y.; Chen, Q.; *J. Alloys Compd.* **2010**, *508*, 546.
DOI: [10.1016/j.jallcom.2010.08.117](https://doi.org/10.1016/j.jallcom.2010.08.117)
33. Liu, L. J.; Fan, H. Q.; Ke, S. M.; Chen, X. L.; *J. Alloys Compd.* **2008**, *458*, 504.
DOI: [10.1016/j.jallcom.2007.04.037](https://doi.org/10.1016/j.jallcom.2007.04.037)
34. Shi, J. H.; Yang, W. M.; *J. Alloys Compd.* **2009**, *472*, 267.
DOI: [10.1016/j.jallcom.2008.04.038](https://doi.org/10.1016/j.jallcom.2008.04.038)
35. Zhou, C. R.; Liu, X. Y.; Li, W. Z.; *Mater. Res. Bull.* **2009**, *44*, 724.
DOI: [10.1016/j.materresbull.2008.09.046](https://doi.org/10.1016/j.materresbull.2008.09.046)
36. Fu, P.; Xu, Z. J.; Chu, R. Q.; Li, W.; Zang, G. Z.; Hao, J. G.; *Mater. Des.* **2010**, *31*, 796.
DOI: [10.1016/j.matdes.2009.07.056](https://doi.org/10.1016/j.matdes.2009.07.056)
37. Chen, M.; Xu, Q.; Kim, B. H.; Ahn, B. K.; Ko, J. H.; Kang, W. J.; Nam, O. J.; *J. Eur. Ceram. Soc.* **2008**, *28*, 843.
DOI: [10.1016/j.jeurceramsoc.2007.08.007](https://doi.org/10.1016/j.jeurceramsoc.2007.08.007)
38. Xu, Q.; Huang, D. P.; Chen, M.; Chen, W.; Liu, H. X.; Kim, B. H.; *J. Alloy. Compd.* **2009**, *471* 310.
DOI: [10.1016/j.jallcom.2008.03.078](https://doi.org/10.1016/j.jallcom.2008.03.078)
39. Xu, Q.; Chen, S.; Chen, W.; Wu, S.; Lee, J.; Zhou, J.; Sun, H.; Li, Y.; *J. Alloy. Compd.* **2004**, *381*, 221.
DOI: [10.1016/j.jallcom.2004.02.057](https://doi.org/10.1016/j.jallcom.2004.02.057)
40. Arlt, G.; Henning, D.; With, G. De; *J. Appl. Phys.* **1985**, *58*, 1619.
DOI: [10.1063/1.336051](https://doi.org/10.1063/1.336051)
41. Zuo, R.; Su, S.; Wu, Y.; Fu, J.; Wang, M.; Li, L.; *mater. Chem. Phys.* **2008**, *110*, 311.
DOI: [10.1016/j.matchemphys.2008.02.007](https://doi.org/10.1016/j.matchemphys.2008.02.007)
42. Kumari, K.; Prasad, K.; Yadav, K. L.; Sen, S.; *Brazilian J. Phys.* **2009**, *39*, 297.
DOI: [10.1590/S0103-97332009000300010](https://doi.org/10.1590/S0103-97332009000300010)
43. Lu, W.; Wang, Y.; Fan, G.; Wan, X.; Liang, F.; *J. Alloy. Compd.* **2011**, *509*, 2738.
DOI: [10.1016/j.jallcom.2010.10.041](https://doi.org/10.1016/j.jallcom.2010.10.041)
44. F. Xia, X. Yao, *J. Mater. Sci.* **1999**, *34*, 3341.
DOI: [10.1023/A:1004672813514](https://doi.org/10.1023/A:1004672813514)
45. Lily; Kumari, K.; Prasad, K.; Yadav, K. L.; *J. Mater. Sci.* **2007**, *42*, 6252.
DOI: [10.1007/s10853-006-0824-y](https://doi.org/10.1007/s10853-006-0824-y)
46. Impedance Spectroscopy Emphasizing Solid Materials and Systems, *J. Ross Macdonald (Ed.)*, Wiley, New York, **1987**.
47. K. Prasad, K. Kumari, K.P. Chandra, K. L. Yadav, S. Sen, *Materials Science-Poland*, **2009**, *27*, 373.
48. Selvasekarapandian, S.; Vijaykumar, M.; *Mater. Chem. Phys.* **2003**, *80*, 29.
DOI: [10.1016/S0254-0584\(02\)00510-2](https://doi.org/10.1016/S0254-0584(02)00510-2)

Advanced Materials Letters

Publish your article in this journal

ADVANCED MATERIALS Letters is an international journal published quarterly. The journal is intended to provide top-quality peer-reviewed research papers in the fascinating field of materials science particularly in the area of structure, synthesis and processing, characterization, advanced-state properties, and applications of materials. All articles are indexed on various databases including [DOAJ](https://doi.org/10.1016/j.jallcom) and are available for download for free. The manuscript management system is completely electronic and has fast and fair peer-review process. The journal includes review articles, research articles, notes, letter to editor and short communications.

